High resolution time and frequency domain spectroscopy of solid state laser materials

Szabo, Alex

Publisher's version / Version de l'éditeur:

Lasers '80: Proceedings of the International Conference, December 15-19, 1980, New Orleans, LA, USA, pp. 374-382, 1981

REPRINTED FROM PROCEEDINGS OF THE INTERNATIONAL CONFERENCE ON LASERS '80, DECEMBER 15-19, 1980

HIGH RESOLUTION TIME AND FREQUENCY DOMAIN SPECTROSCOPY OF SOLID STATE LASER MATERIALS

Alex Szabo
National Research Council of Canada
Ottawa, Canada K1A 0R8

Summary

Frequency and time domain techniques of homogeneous laser spectroscopy of ions in solids are reviewed. Applications in three areas of current interest in our lab are described. These are: resonant energy transfer in ruby, strain characterization of crystals and the possible application of optical hole burning of inhomogeneously broadened lines in solids to a high capacity optical memory.

Introduction

As the development of tunable narrowband lasers over a wide spectral range has progressed, so has our ability to probe, with increasingly high resolution, the spectroscopy and dynamic processes in gases and solids. This paper is concerned with high resolution, homogeneous linewidth studies of low temperature solids using time and frequency domain techniques.

As is well known, ion zero phonon lines[1] in solids are usually inhomogeneously broadened at low temperatures. In crystals, this is mainly due to various kinds of defects[2] which occur on a microscopic as well as a macroscopic scale. While in gases Doppler inhomogeneous broadening could be overcome long before the laser era by using atomic beams[3], overcoming inhomogeneous linewidths in solids has only become possible with the use of lasers. The present optical resolution record[4] in solids is about 2×10^{11} corresponding to a linewidth of 3.1 kHz (FWHM). Having achieved this, what can we do with it?

The first obvious use is for Zeeman[5,6], Stark[7,8], hyperfine[6,9], and stress spectroscopy for which the lines are often not resolved because of inhomogeneous broadening. In addition to the ionically doped inorganic crystal hosts used in refs 5-9, laser line narrowing methods have also been applied to glasses[10], organics[11], and colour centres[12].

Another use is in the study of line broadening mechanisms. In principle, the only limitation on the linewidth at low temperatures should be the excited state lifetime[1], so that for systems such as ruby with a lifetime of 4 msec, we might expect an optical linewidth of $\sim$100 Hz. However observed linewidths are typically much greater[5,13], and some of this was puzzling at first. Part of the problem is a technical one, namely to make very narrow linewidth lasers, however part of the "anomolous" linewidth is real. A principal mechanism in crystals has been found[5,14] to be host nuclear spin interaction which broadens the line by a dynamic Zeeman effect. In glasses, phonon interactions arising from so-called two-level systems have been identified by Prof. Yen's group[10].

Another application is in energy transfer studies. Energy transfer in solids has been much studied, however many phenomena could not be seen with low resolution lamp sources. With high resolution laser excitation, resonant[15] and non-resonant[16] transfer can be studied as well as experimental elucidation of theoretical models of the Anderson transition and mobility edges predicted[17] for inhomogeneously broadened optical transitions in solids.

Techniques

Time Domain

A chronology of the development of the various optical coherent transient techniques is shown in Table I. Historically, our first glimpse of the homogeneous linewidth in a low temperature solid was achieved by Kurnitt, Abella and Hartmann[18] using photon echoes produced by a pulsed laser. Since then, several other techniques have evolved mainly centred about the theme of frequency switching the laser, or the sample by Stark effect. At present, photon echoes are thought to be superior in resolution to free induction decay methods since echoes do not require as high a laser frequency stability[19]. The resolution obtained from time domain methods is presently about two orders of magnitude higher than for frequency domain methods. The reason is simply the short time required to perform the measurement, which means minimal laser jitter.

Table I: Time Domain Techniques for Solids

1. Photon echoes:	Pulsed laser[18]	1964
	Stark shift[7]	1978
	AO frequency shift[19]	1979
	EO phase shift[20]	1979
2. Free induction decay:	Gated CW laser[21]	1973
	Stark shift[7]	1976
	EO frequency shift[22]	1976
	AO frequency shift[23]	1979
	Current resolution[4] $\approx$ 3 kHz	

Frequency Domain Techniques

Table II: Frequency Domain Techniques for Solids

1. Fluorescence line narrowing:	CW & pulsed[5]	1970
	Time-resolved[24]	1975
2. Hole burning:	Photochemical[25]	1974
	Sidebands[26]	1974
	Stark shift[7]	1976
	Two beams[27]	1977
	Burn & sweep[28]	1978
	Polarization[29]	1980

Current resolution[9] $\approx$ 200 kHz

Table II summarizes the development of fluorescence line narrowing (FLN) and hole burning (HB) methods. HB is preferred for the highest resolution and conceptually requires two lasers, one to produce the hole and a tunable laser to probe. Various schemes whereby only one laser is used are embodied in the "sideband","Stark shift" and "burn and sweep" methods listed in Table II.

The basic idea involved in FLN and HB is shown in Fig. 1. If a part of an inhomogeneously broadened line is excited by a narrowband laser, then a narrowed fluorescence line and a hole in the absorption will appear which have twice the homogeneous width. Now for FLN, saturation of the transition is not needed as it is for HB and the question arises as to the power requirement for HB since oscillator strengths in solids are usually quite small (3×10^{-7} for the ruby R_1 line). However, since homogeneous linewidths at low temperature are also quite small, the power requirements for saturation are modest, eg. focussed power of a few microwatts easily produces saturation in ruby[26]. Fig. 2 gives a visual demonstration of optical saturation of the R_1 line in ruby at 4K. The crystal boundaries are shown by the vertical lines (thickness = 4 mm). Two laser beams of the same power are incident from the right. The top beam is unfocussed and is quickly absorbed as it enters the sample. For the focussed beam at the bottom, saturation occurs and the beam goes right through.

Fig. 3 shows a typical FLN set-up. A single frequency laser is tuned into resonance with the transition under study and the line-narrowed fluorescence is spectrally analyzed by a Fabry-Perot. Fig. 4 shows a ruby R_1 FLN spectrum.[30] The spin 1/2 line for this dilute sample is very narrow and is instrument limited at $\sim$ 10 MHz. Echoes[7] say this linewidth should be $\sim$ 200 kHz. The 3/2 line deconvolutes to a width $\sim$ 30 MHz in fair agreement with the limited echo data available[14]. The difference in widths arises from the differing interaction strengths between the host aluminum nuclei and the different Cr^{3+} spin levels[5,14].

As far as ultimate resolution for FLN, Fig. 4 is probably near the limit as determined by the figure of Fabry-Perot plates. To improve on this means going to HB where the only limit is given by the laser frequency stability. It does introduce a difficulty however, in that unlike Lamb dip spectroscopy in gases, two lasers are needed to do HB spectroscopy in solids, one to burn the hole and one to probe. If the hole is long lived, one laser can be used to sequentially burn and probe[28]. For short lived holes, we can't do this and one new scheme developed in our lab[26] for HB spectroscopy is shown in Fig. 5. The basic idea is to weakly amplitude modulate a laser so that the strong carrier can be used to HB and the weak tuneable sidebands are used to probe. Recently, Bjorklund[31] has used FM sidebands for a similar application. In Fig. 5, the transmitted probe is detected by heterodying it with the saturating carrier. With presently available commercial modulators, this scheme is limited to a probe tuning range of 1 GHz which is adequate to observe, for example, rare earth hyperfine structure[9].

Another technique for HB which uses one laser is shown in Fig. 6. Here a fast Stark pulse is applied to the sample to shift the hole through the laser[7,30]. When the hole shifts, the hole shape can be measured as a change in transmitted light through the sample. Fig. 7 shows ruby HB spectra obtained by the Stark technique. Two features to note are that as the intensity increases the hole power broadens and second, which was somewhat of a surprise, the absorption coefficient outside the hole also decreases as the laser intensity increases. This behaviour is due to cross-relaxation in the ground state[30]. The low power linewidth of $\sim$ 2 MHz is largely due to laser frequency jitter.

Resonant Optical Energy Transfer in Ruby

As an example of the use of these techniques, our recent work[32] on energy transfer in ruby will be discussed. Over the past 15 years, there has been much controversy over the question of resonant transfer within the R_1 line in ruby. Based on indirect evidence, most workers believed that transfer rates were fast, 10-1000 $usec^{-1}$. A smaller group favoured much slower rates, $\sim 1\ msec^{-1}$. Associated with this question is whether an Anderson transition[17] occurs in which at sufficiently high concentration ($\sim$ 0.3%), the Cr^{3+} ions switch from a localized to delocalized state with a corresponding increase in transfer rate. Our studies, in which the transfer is directly measured, show two things: first, resonant transfer is slow and second, we see no evidence for an Anderson transition contrary to an earlier claim[33] using another method. The apparatus is shown in Fig. 8 and data as well as the time sequence of the experiment is shown in Fig. 9. The sample is first irradiated for 0.8 msec by a pulse chopped out of a CW dye laser by an acousto-optic modulator. The CW dye laser linewidth is 1 MHz and is resonant with the R_1 line at 6934Å. Right after the laser pulse, a Stark voltage

pulse is applied to the sample for a time τ_c. During τ_c, unexcited Cr^{3+} become resonant with excited ions and start to transfer energy. After the Stark pulse, ions excited by energy transfer are shifted to a new frequency and are detected by time resolved FLN using a boxcar. The FLN spectra in Fig. 9 shows the directly excited line at ν_L and the two transfer peaks at $\nu_L \pm 2S$. The Fabry-Perot resolution is 40 MHz which is sufficient to resolve the homogeneous linewidth of ~ 100 MHz in zero magnetic field.

Now part of this transfer is radiative and part non-radiative. The linear radiative part can be subtracted off to give the non-radiative transfer curves shown in Fig.10. This plots the sum of the transfer peak amplitudes normalized to the directly excited peak vs contact time τ_c for two concentrations. The theoretical curves are obtained using a simple cross-relaxation rate equation model[32]. Reasonable fits are obtained using 1 or 2 different rates of cross-relaxation suggesting that the Cr^{3+} spatial distribution in the crystal is not always microscopically random.

The observed transfer rate is slow, $\sim 1\ msec^{-1}$ for 0.8% ruby. Another feature is that not all of the ions take part in the transfer. Only 5 to 15% transfer as shown by the signal at long times. Also, measurements of the transfer rate vs concentration do not show any sudden jump at the critical concentration of $\sim 0.3\%$ suggested by theory[17] for an Anderson transition. Finally, using the Förster-Dexter theory, calculations show[32] that the observed transfer rate is near that expected for dipole-dipole coupling. The conclusion is that the resonant transfer has an electric multipole origin rather than the earlier believed exchange mechanism.

Another method we have used to search for an Anderson transition is photon echo spectroscopy[34]. In this method, the echo amplitude is measured as the laser is scanned over the inhomogeneous lineshape and we look for a sudden change in amplitude corresponding to a mobility edge. The apparatus is shown in Fig. 11. This shows a new technique for photon echo studies in which two laser pulses are produced by an acousto-optic modulator and the echo is heterodyne detected - using the unshifted beam (which bypasses the sample) as a local oscillator. As discussed elsewhere[34], this scheme has a number of advantages over other echo methods. Fig. 12 shows the result. As can be seen no sharp breaks are observed in the echo scan*. We estimate that at the spectral density at which Khoo et al[33] reported a mobility edge, a change in homogeneous linewidth of ~ 20 kHz out of a total of 700 kHz could have been detected.

Strain Characterization of Crystals

Another application of resonant excitation of crystals we have recently studied is strain characterization. Again, we looked at our old friend ruby with some surprising results. Fig. 13 shows the geometry of the experiment[35] and photographs of the crystal R_1 fluorescence excited by a scanning single frequency CW dye laser. The surprising result is that as the laser frequency is swept, moving regions of fluorescence appear in the crystal indicating large macroscopic strains in our "laser-quality" crystal. Region B looks strain-free and lights up all at once as we tune the laser. However, in region A only about 1/3 of the crystal is resonant at one time. Absorption scans of regions A and B are shown in Fig. 14 and as expected, the linewidth appears much narrower in region B than region A. It is clear that absorption scanning is not a good method for measuring inhomogeneous widths and that serious errors in dipole moment (and other measurements[35]) can occur.

A simple way to overcome these gross macroscopic strain effects on lineshapes is to look at fluorescence from a small volume of the crystal[36]. The improved resolution that results is demonstrated in Fig. 15 which shows the R_1 line structure observed by fluorescence detection as the laser is scanned over the line. A rather narrow inhomogeneous linewidth is seen, 1.2 GHz, which allows for the first time, a clear resolution of the isotope structure.

Optical Memories

The final topic to be discussed is the possible use of HB for a high capacity optical memory[37,38]. The basis of this idea might be stated as follows. Since the large information capacity of laser transmitters is due to the large available bandwidth, then to store large amounts of information using light, we need to store bandwidth or, in other words, have a memory medium which is colour sensitive. Optical HB of inhomogeneously broadened lines in solids is the only high resolution method I can presently see of doing this.

The method is illustrated by Fig. 1 where a hole in the frequency dimension can represent 1 bit of information. In order to avoid cross-talk between holes, an obvious major requirement is that energy transfer, both spatial and spectral, be absent. Another is that the writing power is low and ideally that once written, the holes are permanent. At present, photosensitive organics as first studied by Rebane's group[25] and also Wiersma's group[11], and colour centres[12] look promising.

Various possible realizations of such a memory have been described[37,38]. In one scheme, the storage medium is put in a laser cavity so that it acts as a saturable absorber which allows bistable operation of the laser in various transverse and axial modes. The memory is read by a tunable flood probe beam which falls on a matrix array of diodes. However, for this kind of dynamic memory, there are many practical problems. The main one is the enormous laser power required to maintain the memory if, for example, we tried to use a material like ruby.

* The feature on the right of line centre is due to isotopes.

Something with a much higher cross-section is needed which saturates at lower powers. Also there is no obvious way to erase or flip the bistable state although perhaps a $\pi/2$ pulse could be used for a multilevel system[37]. For the moment, at least, photochemical HB[11,25], which does not require continuous saturation, seems to be the most promising approach[38,39].

As an estimate of the bit density achievable by HB, there are 10^8 spots/cm^2 available spatially as determined by diffraction and for a typical ratio of inhomogeneous to homogeneous width of $\sim 10^6$, this gives a total bit density of 10^{14}/cm^2. This is a factor 100 million times greater than current magnetic hard disc technology. Even if only a fraction of this can be achieved, it's clear that such a fast access, high capacity memory would have an enormous impact on conventional computers and undoubtedly would trigger much thought on new kinds of computer architecture, especially if we also consider the possibility, suggested by many people, of optical logic processing.

In summary, an all optical computer has two compelling arguments in its favour. The large available bandwidth allows many orders of magnitude increase in bit density compared with current schemes and associated with this is the small physical size of the memory which is favourable for high speed. The main battleground will undoubtedly be concerned with heat dissipation. This translates into finding materials with small phonon sidebands which is also useful to minimize cross-talk between holes. Ideally, what we'd like is something like an optical superconductor - a material which has zero dissipative losses associated with its optical transition.

Acknowledgement

The collaboration of P.E. Jessop in parts of the work reported and the technical assistance of E.L. Dimock is gratefully acknowledged.

References

1. R.H. Silsbee, "Optical Properties of Solids", edited by S. Nudelman and S.S. Mitra, Plenum New York 1969, p. 607.
2. A.M. Stoneham, Rev. Mod. Phys. 41, 82 (1969).
3. A.C. Mitchell and M.W. Zemansky, "Resonance Radiation and Excited Atoms", Cambridge London, 1961.
4. R.M. Shelby and R.M. Macfarlane, Phys. Rev. Lett. 45, 1098 (1980).
5. A. Szabo, Phys. Rev. Lett. 25, 924 (1970); ibid 27, 323 (1971).
6. C. Delsart, N. Pelletier-Allard, R. Pelletier, Phys. Rev. B16, 154 (1976).
7. A. Szabo and M. Kroll, Opt. Comm. 18, 224 (1976); ibid Opt. Lett. 2, 10 (1978).
8. R.M. Shelby and R.M. Macfarlane, Opt. Comm. 27, 399 (1978).
9. L.E. Erickson, Phys. Rev. B16, 4731 (1977).
10. J. Hegarty and W.M. Yen, Phys. Rev. Lett. 43, 1126 (1979); L.A. Riseberg Phys. Rev. Lett. 28, 786 (1972).
11. H. de Vries and D.A. Wiersma, Phys. Rev. Lett. 36, 91 (1976).
12. R.M. Macfarlane and R.M. Shelby, Phys. Rev. Lett. 42, 788 (1979).
13. I.D. Abella, N.A. Kurnitt and S.R. Hartmann, Phys. Rev. 141, 391 (1966).
14. D. Grischkowsky and S.R. Hartmann, Phys. Rev. B2, 60 (1970); L.Q. Lambert, Phys. Rev. B7, 1834 (1973).
15. P.E. Jessop and A. Szabo, Phys. Rev. Lett. 45, 1712 (1980); S. Chu, H.M. Gibbs, S.L. McCall and A. Passner, Phys. Rev. Lett. 45, 1715 (1980).
16. P.M. Selzer, D.S. Hamilton and W.M. Yen, Phys. Rev. Lett. 38, 858 (1977).
17. S.K. Lyo, Phys. Rev. B3, 3331 (1971).
18. N.A. Kurnit, I.D. Abella and S.R. Hartmann, Phys. Rev. Lett. 13, 564 (1964).
19. R.M. Macfarlane, R.M. Shelby and R.L. Shoemaker, Phys. Rev. Lett. 43, 1726 (1979).
20. A.Z. Genack, D.A. Weitz, R.M. Macfarlane, R.M. Shelby and A. Schenzle, Phys. Rev. Lett. 45, 438 (1980).
21. P.F. Liao and S.R. Hartmann, Phys. Lett. 44A, 361 (1973).
22. A.Z. Genack, R.M. Macfarlane and R.G. Brewer, Phys. Rev. Lett. 37, 1078 (1976).
23. R.G. DeVoe, A. Szabo, S.C. Rand and R.G. Brewer, Phys. Rev. Lett. 42, 1560 (1979).
24. R. Flach, D.S. Hamilton, P.M. Selzer and W.M. Yen, Phys. Rev. Lett. 35, 1034 (1975).
25. A. Gorokhovski, R.K. Kaarli and L.A. Rebane, JETP Lett. 20, 216 (1974).
26. A. Szabo, IEEE J. Quant. Elect. QE-10, 747 (1974); ibid Phys. Rev. B11, 4512 (1975).
27. C. Delsart, N. Pelletier-Allard and R. Pelletier, Appl. Phys. Lett. 31, 443 (1977).
28. R.M. Shelby and R.M. Macfarlane, Optics Comm. 27, 399 (1978).
29. M.D. Levenson, R.M. Macfarlane and R.M. Shelby, Phys. Rev. B22, 4915 (1980).
30. P.E. Jessop, T. Muramoto and A. Szabo, Phys. Rev. B21, 926 (1980).
31. G.C. Bjorklund, Opt. Lett. 5, 15 (1980).
32. P.E. Jessop and A. Szabo, Phys. Rev. Lett. 45, 1712 (1980).
33. J. Koo, L.R. Walker and S. Geschwind, Phys. Rev. Lett. 35, 1669 (1975).
34. P.E. Jessop and A. Szabo, (to be published).
35. P.E. Jessop and A. Szabo, Appl. Phys. Lett. 37, 510 (1980).
36. P.E. Jessop and A. Szabo, Opt. Comm. 33, 301 (1980).
37. A. Szabo, US Patent 3,896,420 (1975).
38. G. Castro, D. Haarer, R.M. Macfarlane and H.D. Trommsdorf, US Patent 4,101,976 (1978).
39. G.C. Bjorklund (Proceedings of this conference).

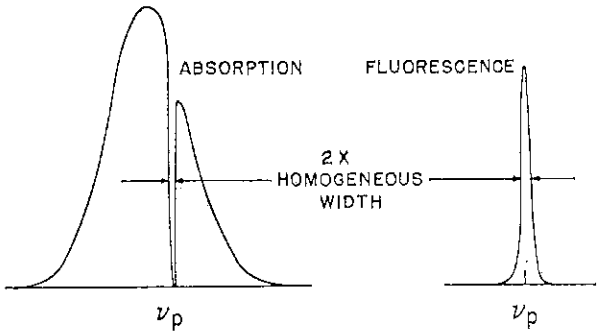

Fig. 1 Fluorescent line narrowing and hole burning in a inhomogeneously broadened line by a narrowband laser.

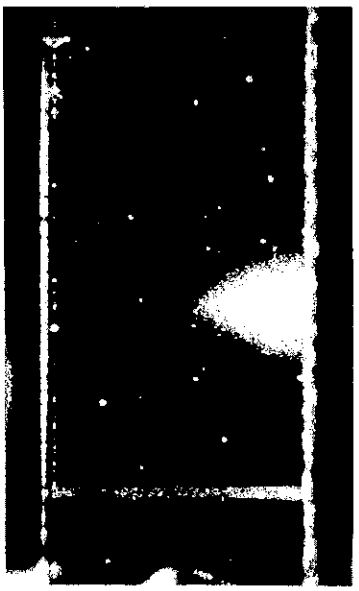

Fig. 2 Visual demonstration of optical saturation in the R_1 line of ruby at 4K (see text).

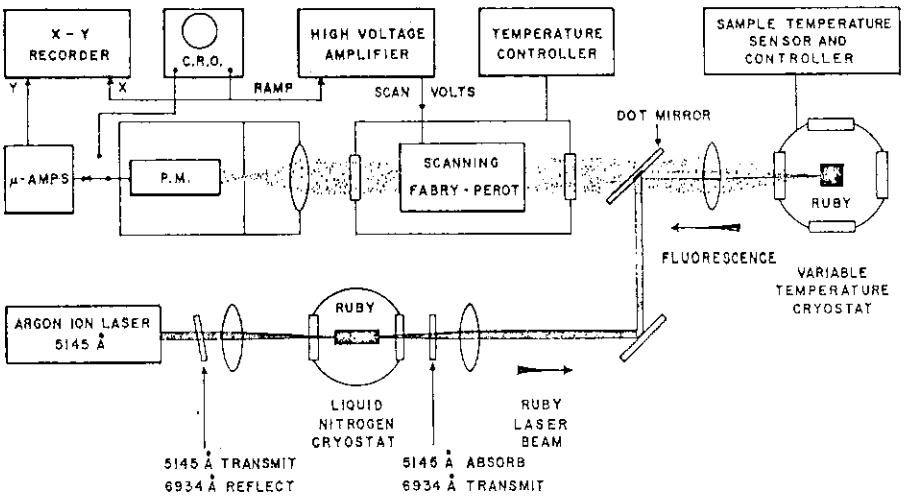

Fig. 3 Apparatus for fluorescence line narrowing.

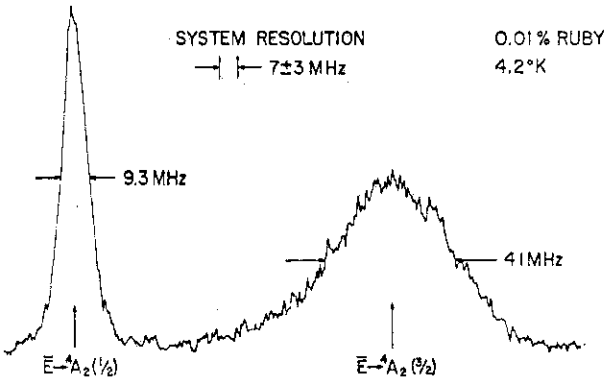

Fig. 4 Ruby R_1 line narrowed spectra in a field ~ 400 gauss along the c axis[30]

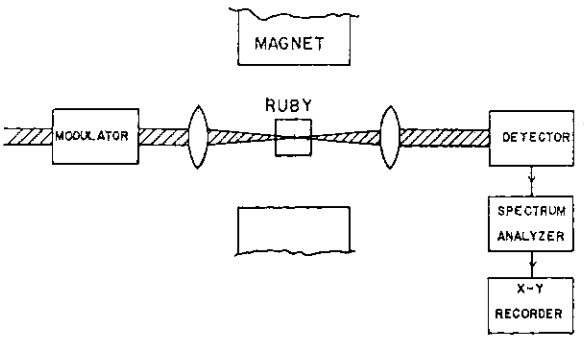

Fig. 5 Apparatus for sideband hole burning spectroscopy[26]

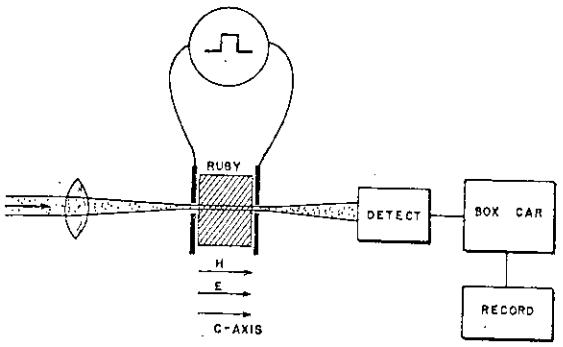

Fig. 6 Apparatus for Stark shifting hole burning spectroscopy[30]

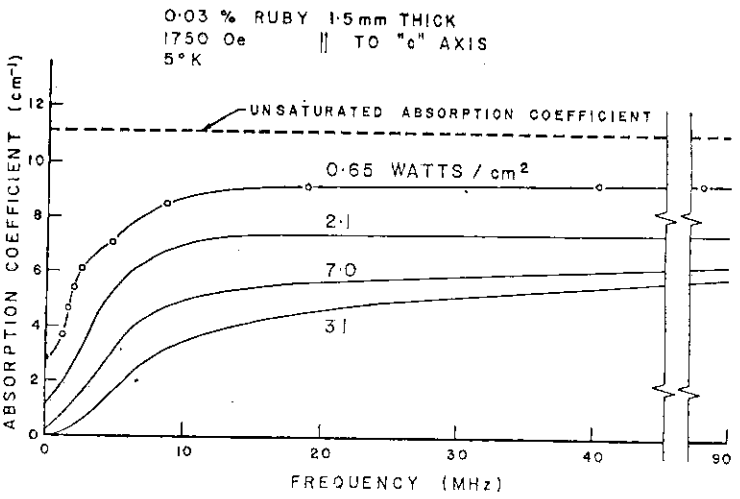

Fig. 7 Ruby hole burning spectra using Stark technique[30]

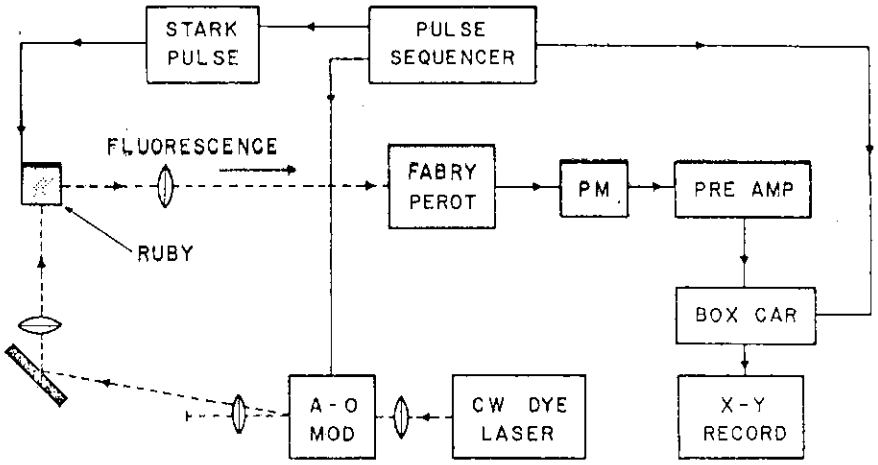

Fig. 8 Apparatus for resonant optical energy transfer studies (see text)

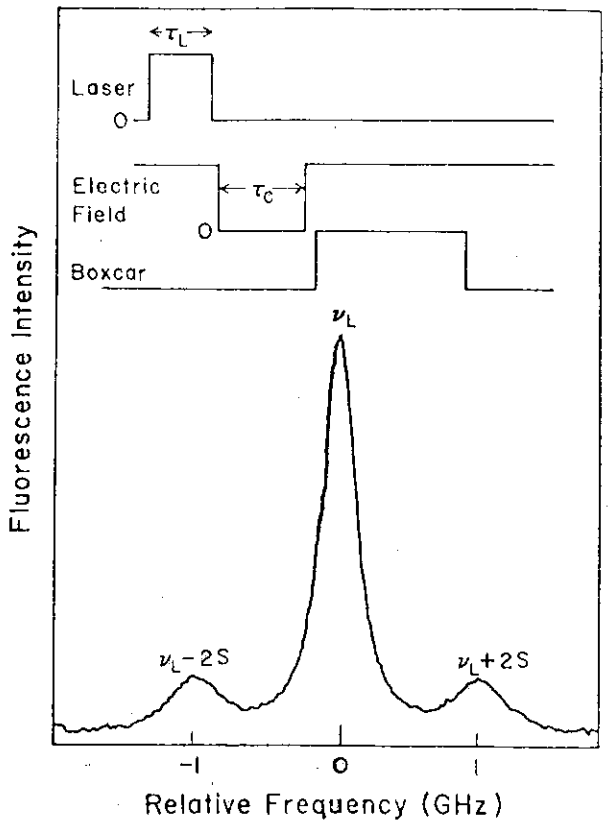

Fig. 9 Fluorescence line narrowing signal showing transfer lines at $\nu_L \pm 2S$ and directly excited line at the laser frequency in 0.37 wt % Cr_2O_3 ruby. Inset shows measurement time sequence.

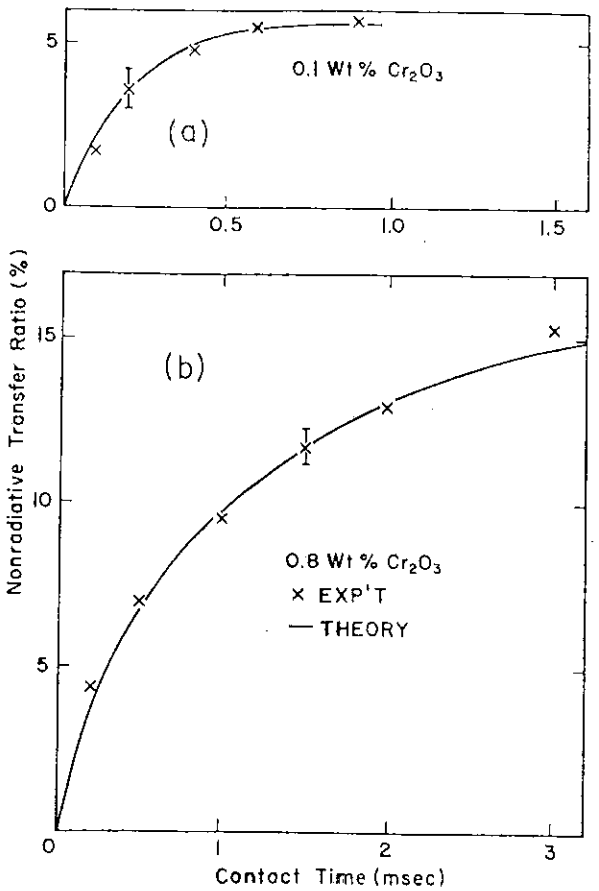

Fig. 10 Time dependence of non-radiative resonant energy transfer in ruby[32]

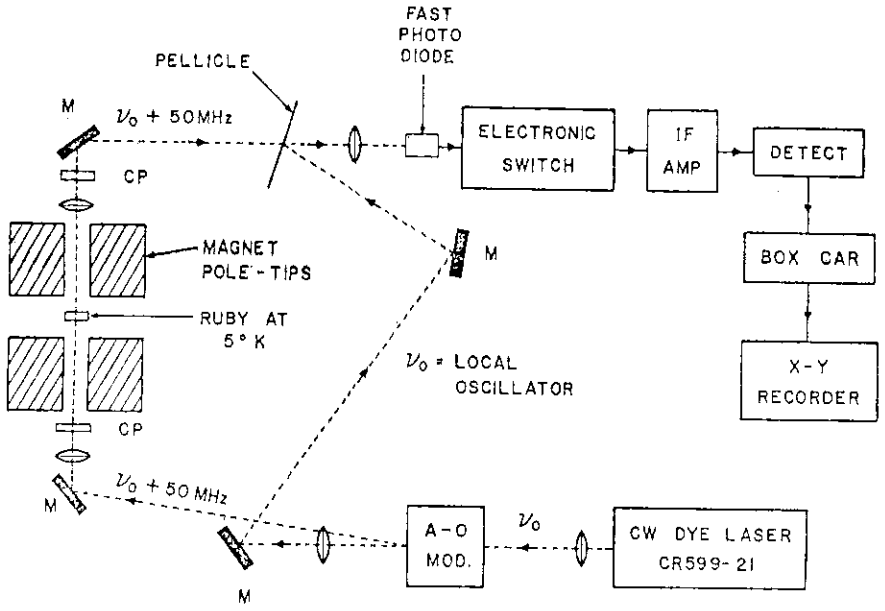

Fig. 11 Apparatus for photon echo spectroscopy.

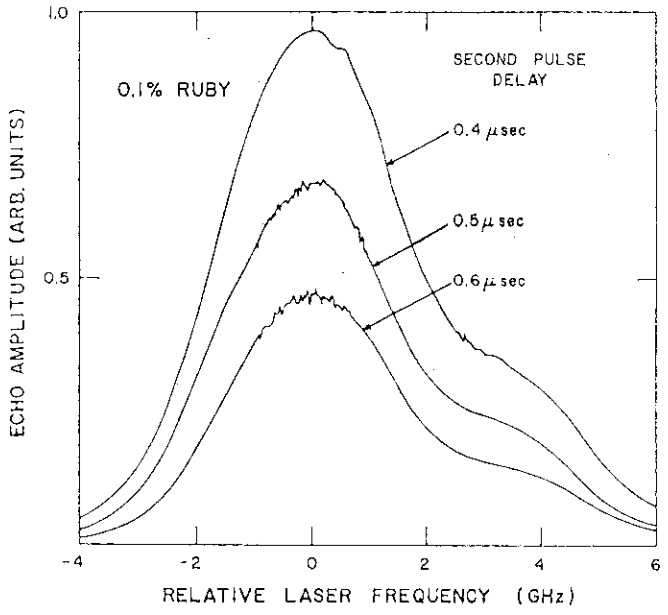

Fig. 12 Photon echo amplitude in ruby, as laser is scanned over the inhomogeneous R_1 line, for various pulse decays.

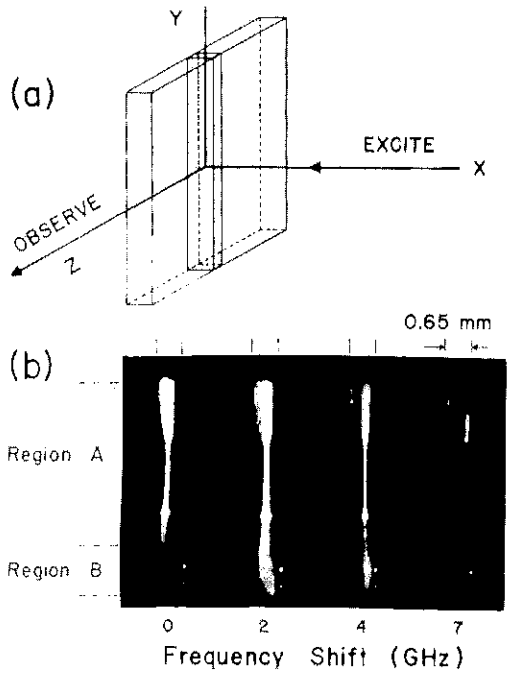

Fig. 13(a) Geometry of laser excitation and viewing. The crystal C_3 axis is along the x axis; (b) R_1 fluorescence photographs of 0.1% Czochralski ruby at 5K vs laser tuning over R_1 line. The crystal is 0.65 mm thick[36]

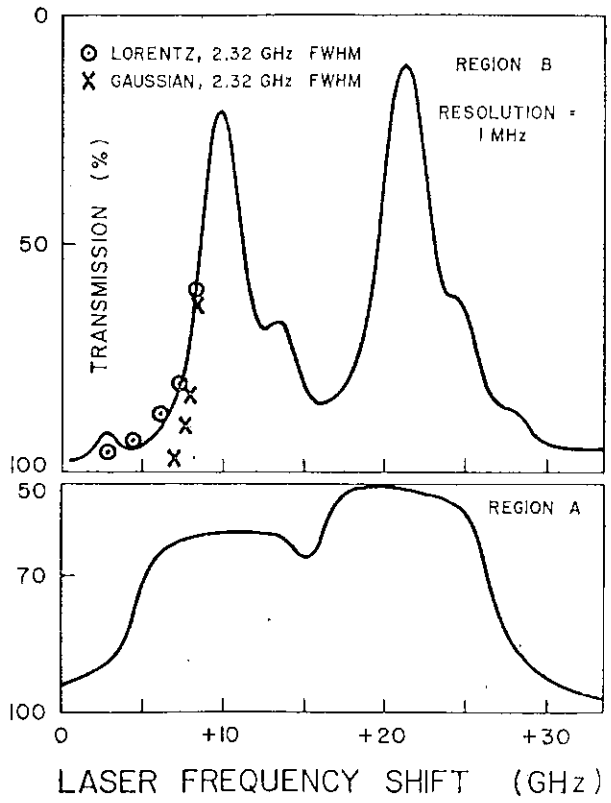

Fig. 14 Absorption scans of regions A and B of Fig. 13 over the R_1 line[36]

Fig. 15 Resonance fluorescence excitation of the R_1 line in ruby. The various isotopic lines are also labeled by their ground state spin quantum number[37]